Observation of Helically-Trapped Energetic Particle Transport Induced by Energetic-Ion-Driven Resistive Interchange Mode using Imaging Neutral Particle Analyzer in Large Helical Device

W. Paenthong[1], K. Ogawa[1,2], S. Sangaroon[3], X.D. Du[4], D. Liu[4], H. Nuga[2], R. Seki[2], H. Yamaguchi[1,2], L.Y. Liao[1], A. Wisitsorasak[5], T. Onjun[6], and M. Isobe[1,2,3]

[1] *The Graduate University for Advanced Studies, SOKENDAI, Toki, Japan*

[2] *National Institute for Fusion Science, National Institutes of Natural Sciences, Toki, Japan*

[3] *Mahasarakham University, Dept. of Phys, Maha Sarakham, Thailand*

[4] *General Atomics, San Diego, U.S.*

[5] *King Mongkut's University of Technology Thonburi, Bangkok, Thailand*

[6] *Thailand Institute of Nuclear Technology (Public Organization), Bangkok, Thailand*

1. Introduction

Energetic-ion-driven resistive interchange mode (EIC) is one of the magnetohydrodynamic (MHD) instabilities [1] that often terminate the sustainment of high ion-temperature plasma in Large Helical Device (LHD) [2]. EIC is excited by a steep pressure gradient of helically-trapped energetic particles (EPs) injected by positive-ion-source-based neutral beam (P-NB), significantly enhancing radial transport, and causing the loss of EPs [3, 4]. Understanding EIC is important for the sustainment of high-temperature plasma in LHD. In this work, we investigate the transport of helically-trapped EPs induced by EIC in LHD using a newly developed Imaging Neutral Particle Analyzer (INPA) [5]. This setup provides spatially and energy-resolved measurements of energetic neutral flux with time resolution. This paper shows the change of energy and radial distribution of charge exchanged energetic neutral flux due to EIC.

2. Experimental Setups

The experiments were performed on hydrogen plasma discharges in LHD, which is one of the largest stellarators in the world with a major radius R of 3.9 m and average minor radius a of ~0.6 m. In these experiments, the toroidal magnetic field strength B_t was set to 2.75 T in the counter-clockwise (CCW) direction viewing from the top, with a magnetic axis position in vacuum R_{ax} = 3.6 m. LHD is equipped with five neutral beam injections: three tangential negative-ion-source-based neutral beam injections (N-NBs) and two P-NBs for plasma heating and the generation of EP, as shown in Figure 1(a). The N-NBs operate with hydrogen

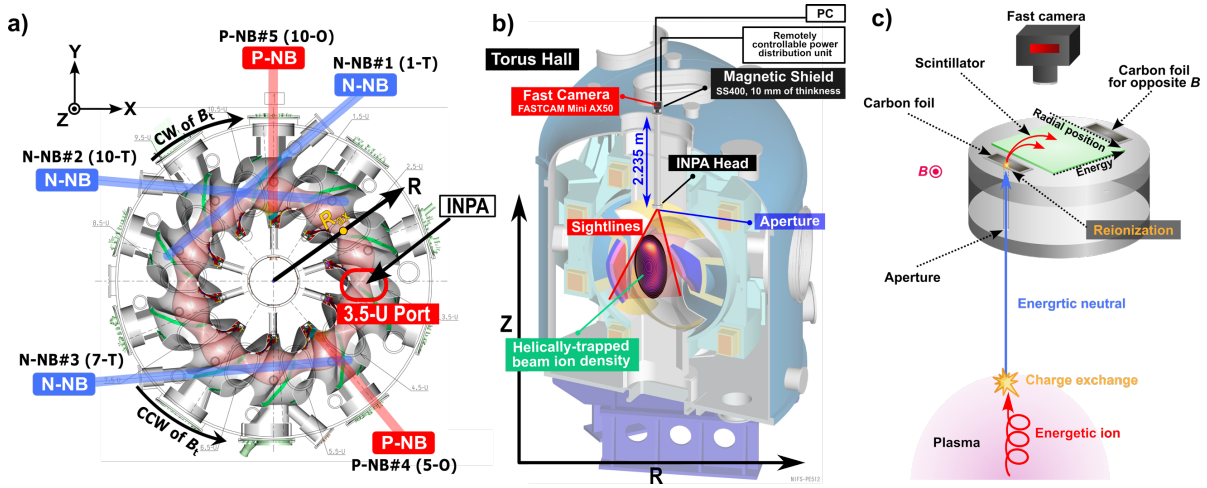

Fig 1. (a) Top view of the LHD showing the arrangement of N-NBs and P-NBs and the location of the INPA, positioned at the 3.5-U port. (b) Schematic of INPA system, installed on LHD. (c) Drawing of the INPA principle.

injection energies of up to 190 keV, while the P-NBs operate with hydrogen injection energies of ~ 40 – 60 keV. The injection power of the N-NBs is approximately 15 MW, while the P-NBs deliver around 10 MW. Beam ions injected by the N-NBs have a typical pitch angle of around 30°, resulting primarily in passing orbits, whereas the ions injected by the P-NBs, with a pitch angle near 90°, mainly have helically-trapped orbits. A steep radial pressure gradient of helically-trapped EP excites the m/n = 1/1 EIC, where m and n denote the poloidal and toroidal mode numbers, respectively, in high-ion-temperature discharges conducted under the relatively low-density conditions.

INPA works as a magnetic spectrometer, measuring two-dimensional, energy-resolved spatial profiles of charge-exchanged neutral particles escaping from the plasma. Energetic neutrals are reionized by a carbon foil and are subsequently deflected by the local magnetic field toward the scintillator, where their bombardment on scintillator induces an illumination pattern. Figure 1 shows the arrangement of the INPA installed on LHD. The INPA was positioned at the 3.5-U port on LHD and designed to measure helically-trapped EPs, with sightlines covering an entire poloidal cross-section. The INPA head consists of two 90 nm thick carbon foils, two apertures, and a ZnS:Ag scintillator. The distance from the scintillator to the camera is 2.235 m. These patterns are recorded using a fast CMOS camera (FASTCAM Mini AX50, Photron Inc.), offering a maximum frame rate of 2000 fps at full resolution of 1024×1024 pixels. In this experiment, the camera was operated at 60 fps with a 10-ms exposure time at 1024×1024 pixels due to the weak scintillation light.

3. Experimental Results

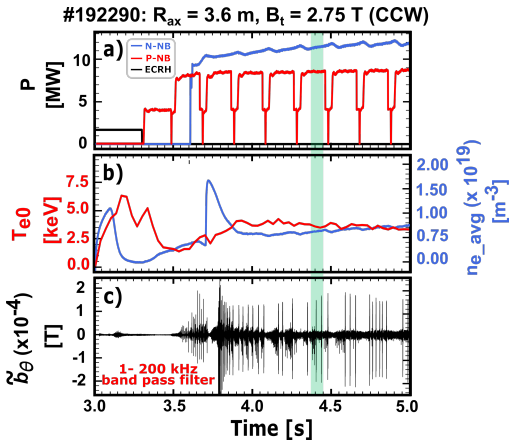

Fig 2. Typical time evolution of plasma discharge #192290 at R_{ax} = 3.6 m and B_t = 2.75 T.

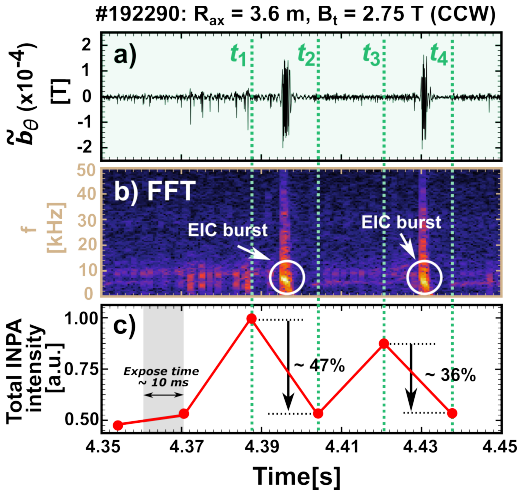

Fig 3. Zoomed time evolution of a plasma discharge showing (a) $\tilde{b}_\theta$, (b) Frequency spectrogram of b_θ, lower than 9 kHz, and (c) total INPA intensity with 10 ms exposure time.

Figure 2 shows the typical time evolution of a high-ion-temperature experiment. The injection power of N-NBs, P-NBs, and Electron Cyclotron Resonance Heating (ECRH), which was used to set up the plasma. The central electron temperature T_{e0} of ~ 3 keV, measured by Thomson scattering diagnostic [6], the line-averaged electron density n_{e_avg} of ~ 0.8×10^{19} m^{-3}, measured with a multi-channel far-infrared laser interferometer [7], and the magnetic fluctuation amplitude ($\tilde{b}_\theta$) obtained by the Mirnov-coil located on the vacuum vessel [8] with 1 kHz to 200 kHz frequency band. Figure 3 presents the zoomed-in time evolutions of $\tilde{b}_\theta$ with 1 kHz to 50 kHz frequency band along with its corresponding frequency spectrogram and the total INPA intensity, defined as the sum over all pixels within each camera frame. During the first EIC burst, the total INPA intensity drops by 47 % between t_1 and t_2; After the second EIC burst, it falls by 36 % between t_3 and t_4. Figures 4 a, b, d, and e present two-dimensional INPA signal distributions in (R, E) space before and after each EIC burst. Before EIC burst (Figs. 4a, d), the emission peak appears at $R \approx 3.85$ m and $E \approx 40$ keV. After EIC bursts (Figs. 4b, e), the intensity is substantially reduced. Figures 4c and f show the differential INPA intensity maps before and after the EIC burst, $\Delta I_{INPA} = I_{INPA,\,before} - I_{INPA,\,after}$. A positive ΔI_{INPA} is observed almost the entire region, whereas a negative ΔI_{INPA} appears in $R < 3.5$ m and $R > 3.9$ m, suggesting outward transport of EPs.

4. Summary

The helically-trapped EP transport induced by EIC was investigated by the INPA in LHD. During EIC burst, total INPA intensity significantly reduced up to 47 %. The change of spatial and energy distribution of energetic neutral flux suggests enhanced transport of EPs due to

EIC. In future work, numerical simulation of INPA signal based on the orbit-following models including the EIC fluctuation will be performed to investigate how EIC affects EP distribution.

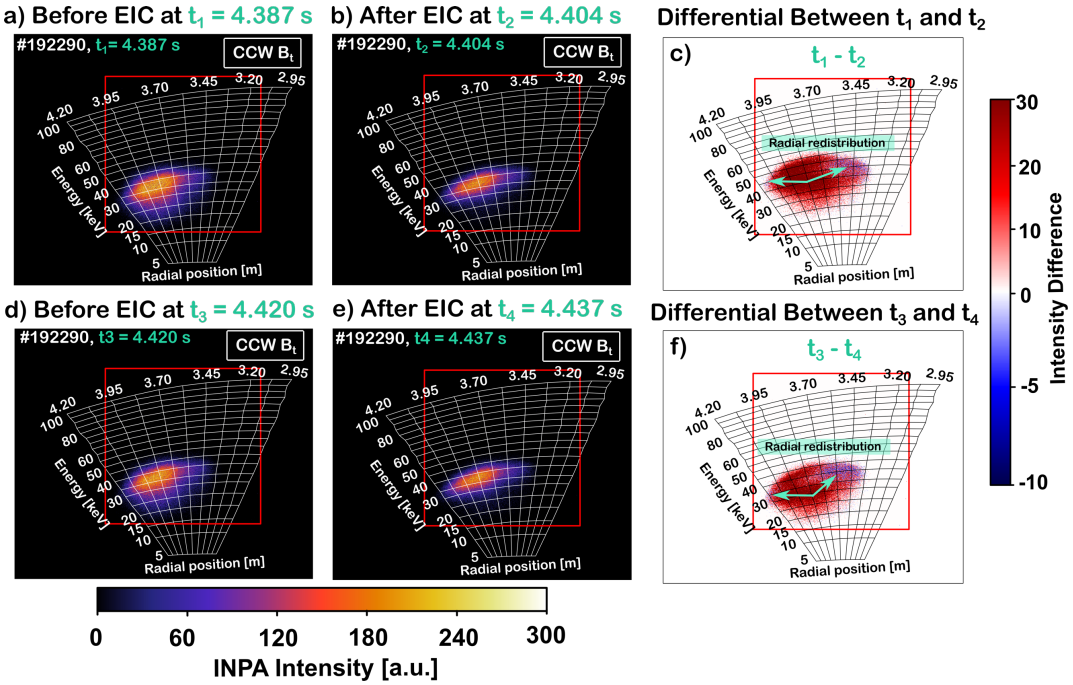

Fig 4. Two-dimensional INPA image for plasma discharge #192290 shown before and after EIC bursts. (a) and (b) comparison of the distribution at $t_1 = 4.387$ s and $t_2 = 4.404$ s of the first EIC burst, (c) and (d) show the corresponding time $t_3 = 4.420$ s and $t_4 = 4.437$ s of the second EIC burst. The color scale indicates the strength of the INPA intensity. Differential INPA intensity maps showing the change in INPA signal between (a) before- and (b) after EIC burst.

References

[1] X. D. Du, *et al*., Phys. Rev. Lett. **114** 155003 (2015).

[2] H. Takahashi *et al.,* Nucl. Fusion **58** (2018)106028.

[3] K. Ogawa, *et al*., Nucl. Fusion **58** 044001 (2018).

[4] K. Ogawa, *et al*., Nucl. Fusion **60** 112011 (2020).

[5] W. Paenthong, *et al*., Rev. Sci. Instrum. **95** 083547 (2024).

[6] I. Yamada, *et al*., Fusion Sci. Technol. **58** 345 (2010).

[7] T. Akiyama, *et al*., Fusion Sci. Technol. **58** 352 (2010).

[8] S. Sakakibara, *et al*., Fusion Sci. Technol. **58** 471 (2010).

Acknowledgments

We are pleased to acknowledge the assistance of the LHD Experiment Group. This work was partly supported by the NINS program of Promoting Research by Networking among Institutions (Grant Number 01412302) and the Program Management Unit for Human Resources and Institutional Development, Research and Innovation (grant number B39G670014).